Numerical Model for Characteristic Curves of Photothermographic Materials Using a Semiempirical Simulation Method

Tsukasa Ito,▲* Shu Nishiwaki† and Tsuyoshi Mitsuhasi†

**CM R&D Center, Konica Corporation, Hino-shi, Tokyo, Japan*
†MG Research and Development Center, Konica Corporation, Hino-shi, Tokyo, Japan

Photothermographic materials that contain silver halide grain and organic silver salts are widely used in dry processing imaging systems. Because its characteristic curves are very sensitive to development condition, precise calculations of the characteristic curves under various development conditions are essential for practical development system designing. Though some previous models for the characteristic curves had been proposed, those uses are limited because they based on some ideal assumptions. In this study, change of experimental characteristic curves under various development conditions was analyzed, and a new model using semiempirical simulation method was found. This method gives both the fraction of silver halide grains receiving a latent image exposure and the radius of sphere of influence from the experimental characteristic curves of several development conditions. The fraction is an intrinsic value of the film, and it represents the photosensitive character including fog. The radius of sphere of influence represents the degree of development, and its rate of increase is constant under fixed development temperature. These parameters are useful for analysis of development rate. Once these parameters were defined, exact characteristic curves of any development conditions are calculable. The found simulation method is useful for analysis and design of practical photothermographic system.

Journal of Imaging Science and Technology 45: 357–364 (2001)

Introduction

Photothermographic materials that contain silver halide grain and organic silver salts are widely used in dry processing imaging systems. In these systems, latent image centers are formed on the surface of silver halide grains by light exposure. These latent image centers are grown into visible metallic silver image by physical development in thermal development process. Silver ions are supplied from organic silver salts that surround the silver halide grain. In contrast with classical silver halide photography, silver from the silver halide grains doesn't contribute to the developed silver density. So the behavior of its characteristic curve differs from one of classical silver halide photography. Because the characteristic curves of photothermographic materials are very sensitive to its development condition, precise calculations of the characteristic curves under various development conditions are essential for practical development system designing.

Klosterboer and Rutledge[1,2] gave the fundamental theory for calculation of thermally developed characteristic curves. They assume that only the silver from the organic silver salts within a certain radius from a silver halide latent image has the time to diffuse to the latent image and be reduced to image silver during development time. This spherical volume was named *sphere of influence*. These spheres are observed as white faint hollows using a scanning electron microscope. Based on this assumption, they gave a primary numerical model for characteristic curves. In the model, number of latent image centers was calculated from exposure and grain size, based on Poisson's distribution. Amount of developed silver was considered to be equivalent to amount of organic silver salts within the sphere of influence. This amount was calculated from the volume of sphere of influence and the content of organic silver salts. Optical density was assumed to be proportional to the amount of developed silver. Radius of the sphere of influence must be limited so that the volume of the sphere of influence does not exceed the physical layer volume. Their conclusion is summarized in Eqs. 1, 2 and 3. Details of the derivation are mentioned in the Appendix.

Klosterboer and Rutledge's Model

$$f = \left[\sum_{p=m}^{\infty} \left(a \cdot E \cdot L^2\right)^p \frac{e^{-a \cdot E \cdot L^2}}{p!} \right] \tag{1}$$

$$D = \frac{K \cdot f \cdot W_{SS} \cdot A}{\left(T \cdot d / W_{SH}\right) - 1} \left[\left(\frac{4}{3} \pi (r / L)^3 \right) - 1 \right] \tag{2}$$

$$\frac{r}{L} \le \left[\frac{3}{4\pi} \left(\frac{T \cdot d}{W_{SH}} + 1 \right) \right]^{\frac{1}{3}} \tag{3}$$

Original manuscript received September 10, 2000

▲ IS&T Member

where
f: fraction of silver halide grains receiving a latent image exposure
m: number of absorbed photons required forming a latent image
E: number of photons per unit area
a: fraction of photons absorbed
L: edge length of the silver halide grain
D: optical density of the film
K: proportional constant
W_{SS}: coating weight of organic silver salts per unit area
T: thickness of coated layer
A: coated area
d: density of silver halide grains
W_{SH}: coating weight of silver halide grains per unit area
r: radius of sphere of influence

The limitation of Eq. 3 seems to be somewhat unnatural. Though total volume of the sphere of influence should be equal to physical layer volume of the film at the maximum value of r, spheres of the maximum radius couldn't packed into the physical layer without overlapping. In fact, calculated results of their model tend to differ from experimental characteristic curves at shoulder to maximum range.[3,4]

The most important insufficiency in the Klosterboer and Rutledge's model is the implicit assumption that the spheres of influence do not overlap. This suggestion was pointed out by Kong[5] and Hirano[6] in 1997, and they gave improved equations respectively. Also Hirano[6] pointed out further insufficiencies of Klosterboer and Rutledge's model. The points in his argument are as follows.

1. Overlap of the sphere of influence should be considered instead of the limitation of its radius.
2. Optical density is not proportional to the amount of developed silver. Covering power should be considered.
3. Dead volume of the undeveloped silver halide grains within the sphere of influence should be considered.

In Hirano's model, overlap of the sphere of influence was corrected by integration of its probability, and the limitation for the radius of sphere of influence was repealed. Optical density was assumed to be proportional to the shadow area of developed silver particles considering the covering power. And the optical density was calculated from both number and radius of the developed silver particles. The undeveloped silver halide grains incorporated in the sphere of influence were treated as dead volume in calculation of the amount of developed organic silver salts, and the dead volume was calculated from probability of the incorporations. Hirano's model is summarized in Eqs. 1, 4, 5, 6, 7 and 8. Details of the derivation are mentioned in the Appendix.

Hirano's Model

$$N_0 = \frac{W_{SH} \cdot A}{d \cdot L^3} \tag{4}$$

$$N = f \cdot N_0 \tag{5}$$

$$P_{SS} = \frac{W_{SS} \cdot A}{A \cdot T - N_0 \cdot L^3} \tag{6}$$

$$M = P_{SS}\left[AT\left\{1 - \exp\left(-\frac{4}{3}\pi r^3 \frac{N}{AT} \right)\right\} - NL^3 \right]\left(\frac{AT - N_0 L^3}{AT - NL^3} \right) \tag{7}$$

$$D = C \cdot M^{\frac{2}{3}} \cdot N^{\frac{1}{3}} \Big/ A \tag{8}$$

where
N_0: number of total silver halide grains
N: number of silver halide grains receiving a latent image exposure
P_{SS}: content of organic silver salts in the coated layer
M: mass of the developed silver
C: proportional constant for covering power

In both Kong's model and Hirano's model, radius of the sphere of influence could grow without limit, but the amount of developed silver converges on the coating amount because of overlap of the spheres of influence. This treatment seems to be quite an improvement. In 1999 Kong[7] developed a further generalized model in consideration of incomplete reduction of organic silver salts within the sphere of influence, variations in size and shape for the sphere of influence, random distribution of AgX grains, grain-shape and grain-size distribution, and fog centers. Though the model stands on most realistic assumptions, it incorporates too many parameters. To fix all the parameters from experimental data is rather difficult, so methods to fix parameters in part were reported.

Purpose of the Study

On design of a dry processing imaging system, it is very important to keep the shape of characteristic curves under precise control. Because the characteristic curves of photothermographic materials are very sensitive to development conditions, system designers often need to calculate the precise change of the characteristic curves under various development conditions. Some problems must be solved prior to use of the previous models. In Kong's (1997) and Hirano's models, calculation of the fraction of silver halide grains receiving a latent image exposure was based on Poisson's distribution in Eq. 1. This treatment was based on the assumption that silver halide grains are uniform in sensitivity. But in practice, the sizes of grains are distributed, and it is difficult to examine precise distribution of their size because they are very small (about 0.05 μm in edge length). In Kong's (1999) model, the distribution and size of the latent images are determined by Poisson statistics. Though it is a proper approach, to calculate the whole shape of the sensitometric curve is not easy. Additionally, the image density is assumed to be proportional to the amount of developed silver particles in both Kong's models. This is a typical difference from Hirano's model and this study, in which the image density is assumed to be proportional to the shadow area of developed silver particles considering covering power.

Though spheres of influence are observed as white hollows using a scanning electron microscope, their figures are too faint and too distorted to examine distribution of their size. Radius of sphere of influence should be regarded as a conceptual parameter. To solve these problems, we adopt a semiempirical method. In this study, values of the fraction of silver halide grains receiving a latent image exposure, the radius of sphere

TABLE I. Conditions of Thermal Development

No	Heat time (sec.)	Temperature (°C)
1	14	119
2	14	121
3	14	123
4	14	125
5	14	127
6	7	125
7	10	125
(4)	14	125
8	20	125
9	30	125

of influence, and the proportionality constant for covering power are determined systematically from the experimental characteristic curves of various development times and temperatures.

Experimental

Konica Medical Imaging Film SD-P is exposed uniformly, and developed under various development times and temperature. The coating weight of organic silver salts is equivalent to 19 g/m^2 of silver metal, and the coating weight of silver halide grains is equivalent to 1 g/m^2 of silver metal. The average edge length of the silver halide grain is 0.065 micrometer. The thickness of coated layer is 20 micrometer. Both exposure and development were performed by Konica DRYPRO model 722. The wavelength of exposure is 810 nm. The system program was modified to be capable of adjusting development conditions. Table I shows the development conditions.

Results

Figure 1 and 2 show the characteristic curves of various development conditions.

These data were used in following regression analyses. First, Hirano's model equations were modified to suitable form for regression. Equation 1 of Hirano's model was deleted. Instead, f, namely fraction of silver halide grains receiving a latent image exposure was treated as a look up table function in Eq. 9. Their table values were fixed latter. Because Hirano's Eq. 7 has an inconsistency when the volume of a sphere of influence is near to the volume of a silver halide grain, a correction term is added referring to Kong's (1999) model. The detail of the correction is mentioned in the Appendix. Equations 4 to 8 were arranged into one equation by substituting N_0, N, P_{SS}, and M. A was eliminated.

New Model

$$f = g(Ex)\ 0 < f < 1\ Ex:\ \text{exposure} \tag{9}$$

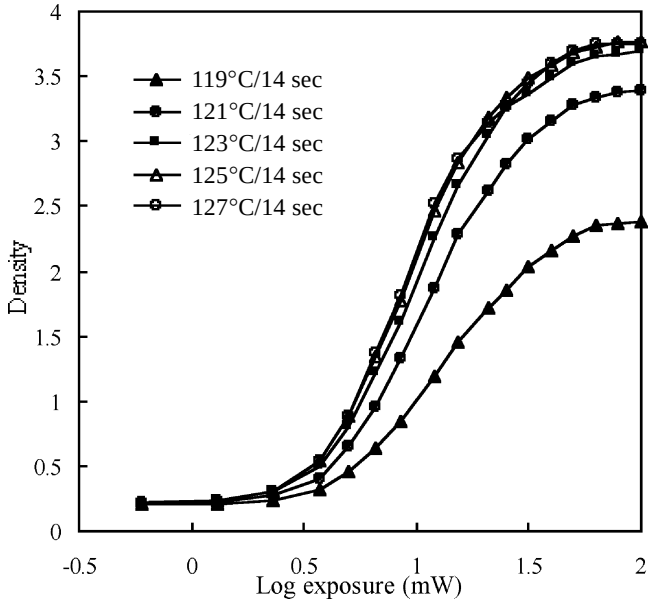

Figure 1. Characteristic curves at various temperatures.

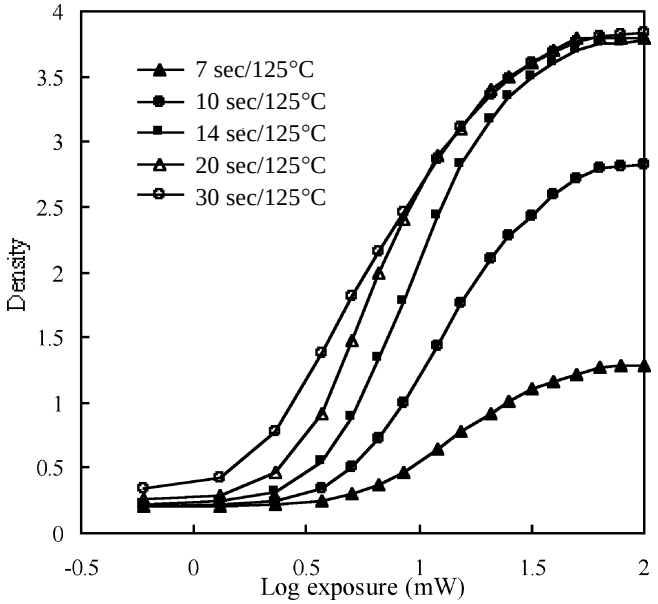

Figure 2. Characteristic curves at various times.

$$D = C \cdot \left[W_{SS} \cdot \frac{f \cdot W_{SH} - T \cdot d \left\{ 1 - \exp\left(-\left(\frac{4}{3} \cdot \pi \cdot r^3 - L^3 \right) \cdot \frac{f \cdot W_{SH}}{T \cdot d \cdot L^3} \right) \right\}}{f \cdot W_{SH} - T \cdot d} \right]^{\frac{2}{3}} \cdot \left[\frac{f \cdot W_{SH}}{d \cdot L^3} \right]^{\frac{1}{3}} \tag{10}$$

TABLE II. The Principal Differences Between Previous Models and This Study

	Klosterboer[2]	Kong (1997)[5]	Hirano[6]	Kong (1999)[7]	This Study
Overlap of the sphere of influence	Ignored	Considered	Considered	Considered	Considered
The image density is proportional to	Amount of Ag	Amount of Ag	Shadow area of Ag	Amount of Ag	Shadow area of Ag
Fog centers	Ignored	Ignored	Ignored	Considered	Considered
Correction for AgX grain volume	Ignored	Ignored	Considered	Considered	Considered
AgX grain-shape, grain-size and sensitivity distributions	Ignored	Ignored	Ignored	Considered	Eliminated
Poisson statistics	Number of latent images	Number of latent images	Number of latent images	Number and size of latent images	Not used
Variations in size and shape for the sphere of influence	Ignored	Ignored	Ignored	Considered	Ignored
Amount of the reduced organic silver salt in the sphere of influence.	All	All	All	Fraction	All

The differences between previous models and this study are summarized in Table II.

Though Eq. 10 is complicated, it can be interpreted as follows.

$$D = h(f,\ r,\ C,\ W_{SH},\ W_{SS},\ L,\ T,\ d) \qquad (10')$$

In this equation, parameter f, r and C are unknown, and their values need to be fixed. The rest, such as coating weight and layer thickness are already known. In Hirano's model, L, namely edge length of the silver halide grain has two functions. First, L impacts the speed of the film in Eq. 1. Second, L represents the volume of the silver halide grains in Eqs. 4, 6 and 7. Differing from Hirano's model, f is independent of L in our model. L only represents the volume of the silver halide grains in Eq. 10. So a rough average value for L is enough for our calculation.

Equation 10 gives a maximum value at f equal 1 and r equal infinity. This represents that the maximum density would be obtained at the condition of sufficient exposure to form a latent image on all silver halide grains and sufficient developing time to consume all organic silver salts. Equation 11 shows the maximum density value.

$$D_{\max} = C \cdot {W_{SS}}^{2/3} \cdot \left(\frac{W_{SH}}{d \cdot L^3}\right)^{1/3} \qquad (11)$$

$$\therefore C = D_{\max} \cdot {W_{SS}}^{-2/3} \cdot \left(\frac{W_{SH}}{d \cdot L^3}\right)^{-1/3} \qquad (12)$$

Parameter C, namely the proportionality constant for covering power was fixed by putting the observed maximum density into Eq. 12. The base density must be subtracted prior to use. To get a proper maximum density, the exposure should be in the range of practical use. Extreme exposure causes the formation of undesired latent image on *in situ* silver halide, and gives excessive density. Now r and f remain to be evaluated. To fix these, an inverse function for Eq. 10 was defined.

$$f = h^{-1}(D,\ r,\ C,\ W_{SH},\ W_{SS},\ L,\ T,\ d) \qquad (13)$$

Though the algebraic expression of above function is difficult to solve, numerical solution of above is calculable by iterative routines such as the Newton–Raphson method. Initial values for f were calculated by putting 1 μm in the place r and putting experimental density (base density was subtracted) of Fig. 1 in the place D on Eq. 13. Figure 3 shows the initial value for f.

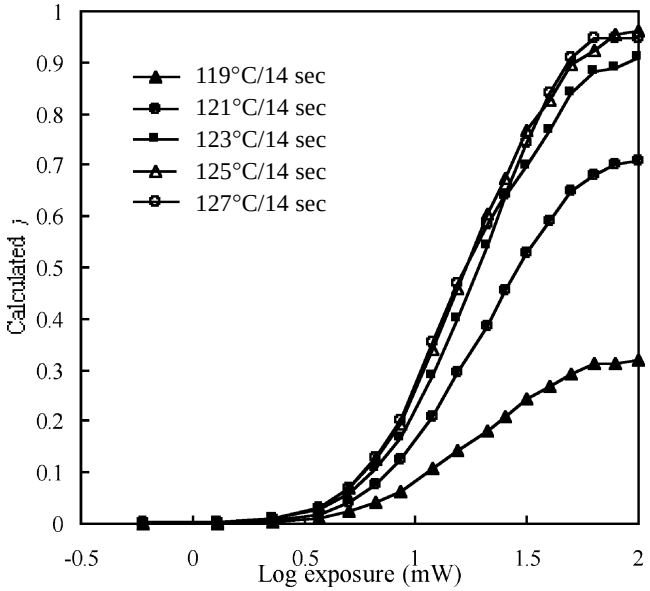

Figure 3. Calculated f for r = 1 μm.

These f values are NOT proper. Because all experiments are equal in the sensitivity and exposure conditions, calculated f, namely the fraction of silver halide grains receiving a latent image exposure should be equal to each other at the same exposure. So all plot lines should gather to almost one line. Because r, namely radius of sphere of influence, is the only undecided parameter in the right hand side of Eq. 13, the value of r should be adjusted to gather all plot lines. This assumption is a key principle of our method. Error function of Eq. 14 was defined for calculation of the optimum r.

$$\overline{D}_i = \frac{1}{n}\sum_{j=1}^{n} D_{i,j} \quad Err = \sum_{j=1}^{n}\sum_{i=1}^{m}\left(D_{i,j} - \overline{D}_i\right)^2 \qquad (14)$$

where

i: wedge index

j: development condition index

D_{ij}: experimental optical density at wedge i and condition j.

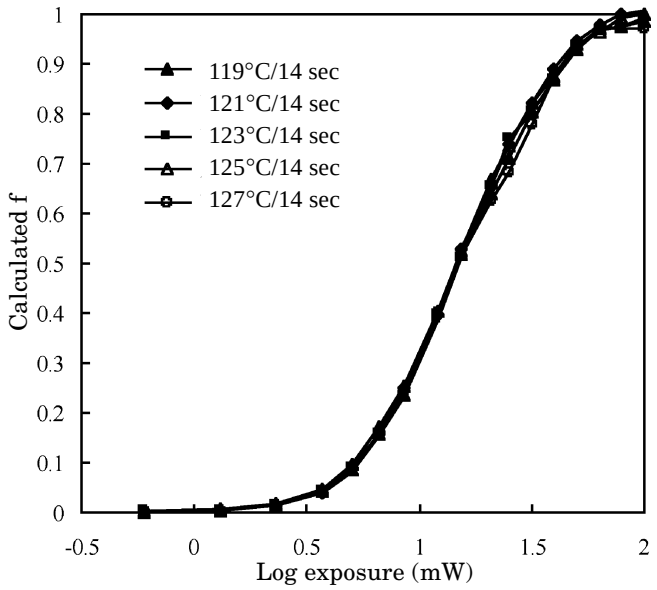

Figure 4. Calculated *f* at optimum *r* values.

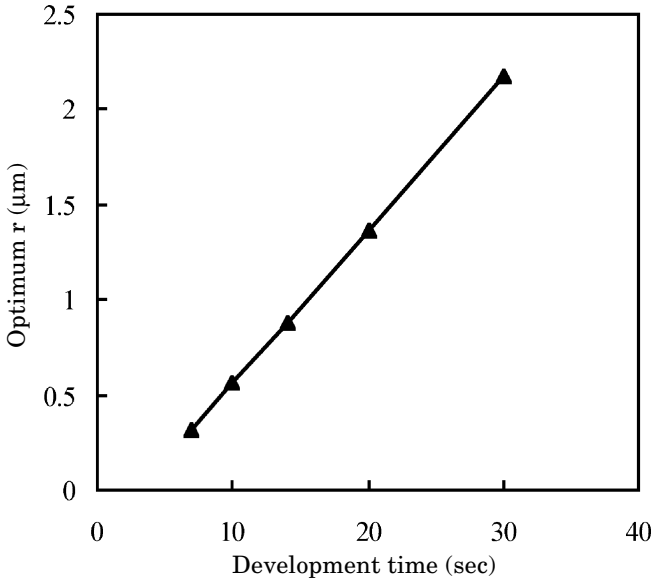

Figure 6. Optimum *r* at various development times.

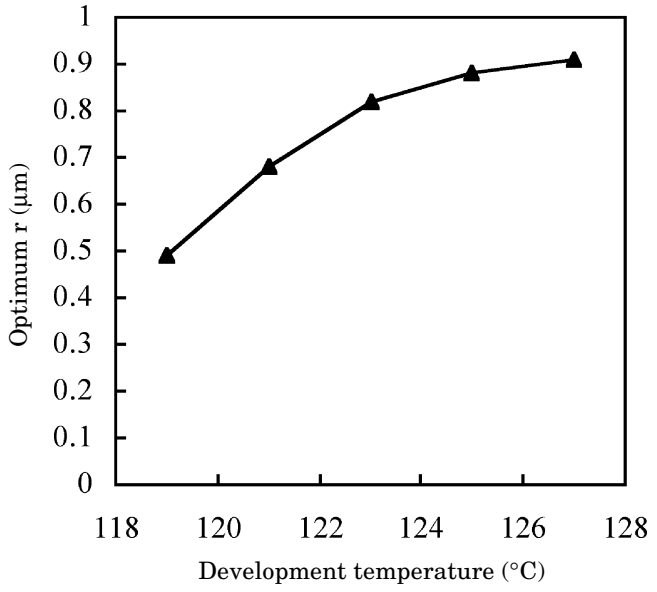

Figure 5. Optimum *r* at various development temperatures.

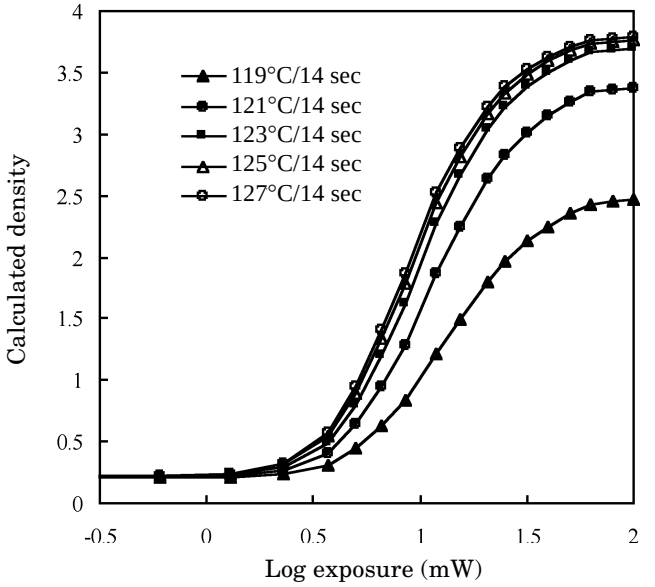

Figure 7. Calculated characteristic curves at various development temperatures.

Parameter *r* for each development condition were adjusted to give minimum *Err* in Eq. 14 using the Marquardt method.[8] Figure 4 shows calculated *f* at optimum *r*.

At optimum *r*, all plot lines gathered in almost one line. This result proves our hypothesis. Average of the calculated *f* in Fig. 4 was adopted as final value for *f*. Characteristic curves of each development conditions were calculated by putting the final value for *f* and the optimum *r* on Eq. 10. Figures 5 and 6 show the optimum *r*. Figures 7 and 8 show the calculated characteristic curves. Figure 9 shows the correlation between experimental fog and calculated fog.

Quite a linear relationship exits between the radius of the sphere of influence and developing time in Fig. 6. Calculated characteristic curves in Figs. 7 and 8 agree well with corresponding experimental characteristic curves in Figs. 1 and 2. Also calculated fog well agrees with experimental fog in Fig. 9.

Discussion

Various features of characteristic curves in Figs. 1 and 2 can be explained by only a change in the value of *r* in Eq. 10 with a common value of *f*. Parameter *f*, namely fraction of silver halide grains receiving a latent image exposure is an intrinsic value of the film, and it represents the photosensitive character of the film. Figure 10 shows relationship between exposures and values of *f*.

At minimum exposure, calculated *f* has a convergence value that is above zero. Experimental fog was explained using this convergence value. This convergence value represents the fraction of silver halide grains having fog centers. Because the development conditions of our

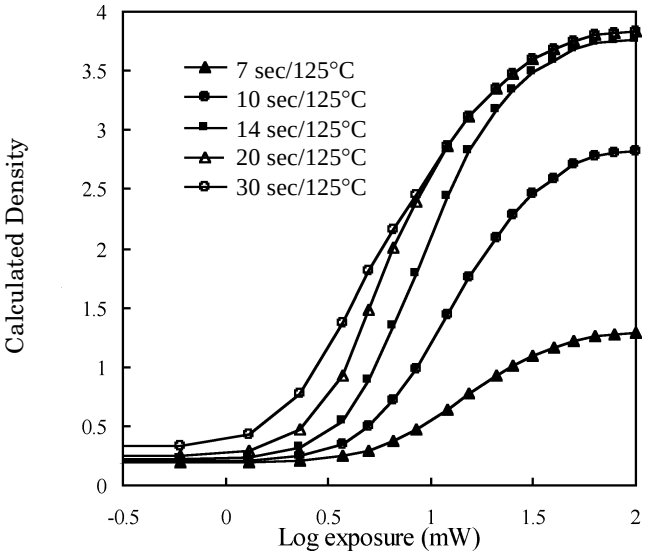

Figure 8. Calculated characteristic curves at various development times.

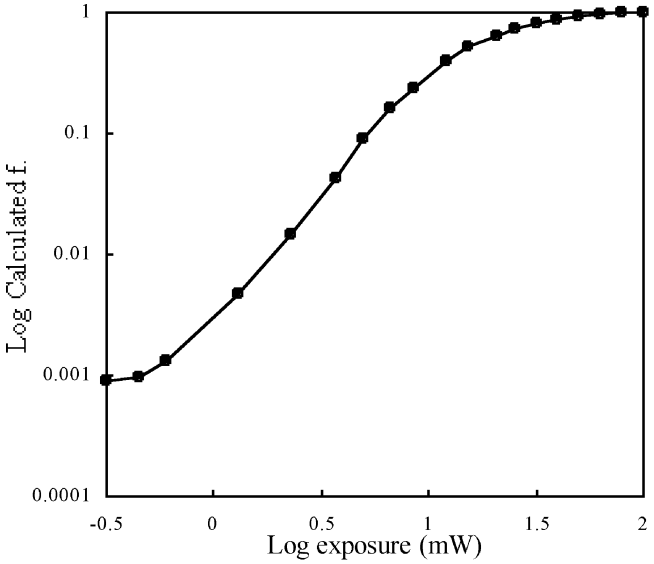

Figure 10. Relationship between exposure and value of *f*.

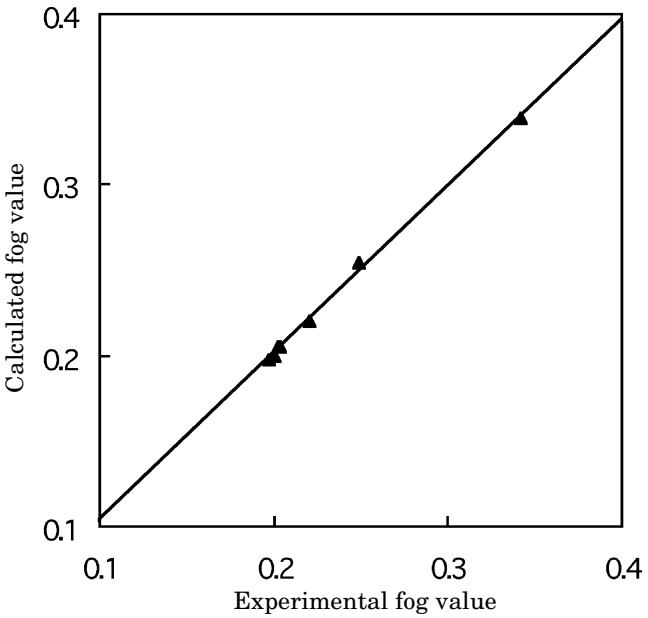

Figure 9. Correlation between experimental fog and calculated fog.

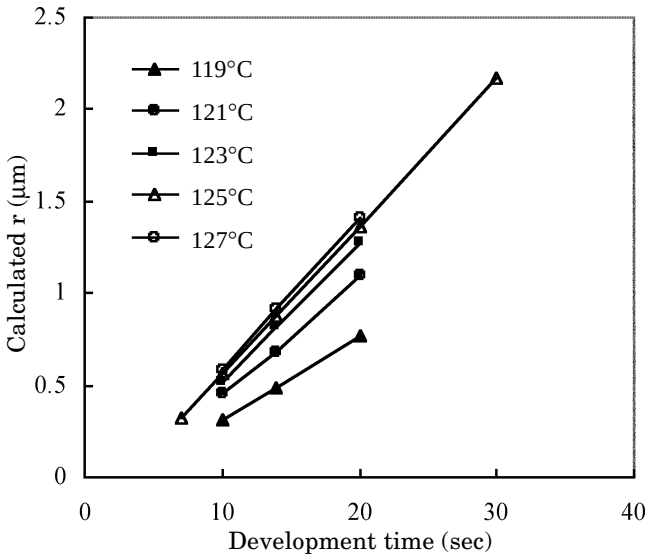

Figure 11. Relationship between *r* and development time at various temperatures.

experiments vary within the range of practical use, the results only suggest that the change of the fraction of silver halide grains having fog centers is negligible in the range of practical development conditions.

Parameter *r*, namely radius of sphere of influence varies with the condition of development. The value should be regarded as a conceptual parameter that indicates the degree of development. It is noteworthy that linear relationship exits between the value of the *r* and the development time in Fig. 6. It implies that the rate of increase of the radius of sphere of influence is constant at a fixed development temperature. The average diffusion length of the silver ion from organic silver salts to the development centers should be proportional to the radius of sphere of influence. So the diffusion rate should not be the rate-determining step of the development reaction. At the early state of development when overlap of the sphere of influence is negligible, the rate of increase of the amount of developed silver is proportional to square of the radius of sphere of influence. It implies that development rate is proportional to the surface area of developed silver or of the sphere of influence. At the late stage of development, the corresponding rate rapidly decreased owing to overlap of the spheres of influence. In Fig. 6, the *x* axis intercept probably represents the heating time before the film temperature increased enough to initiate development.

The increasing rate of *r* should be regarded as a parameter that indicates development rate, which depends on development temperature. Figure 11 shows the relationship between *r* and development time, including additional data at various development temperatures.

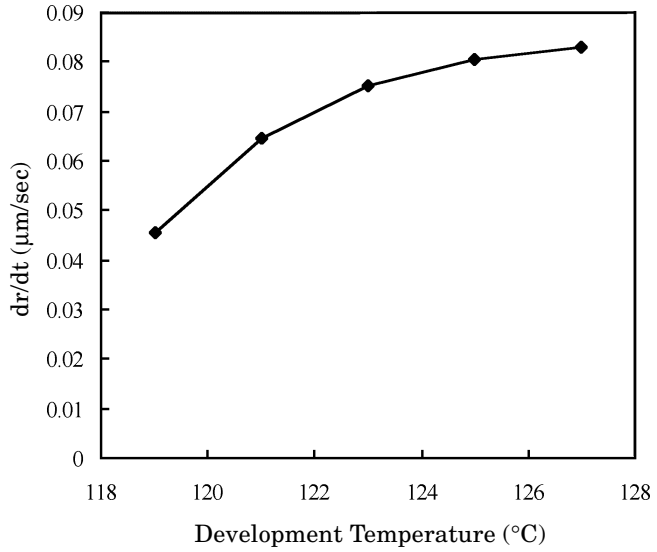

Figure 12. Relationship between rate of increase of r and development temperature.

Figure 12 shows relationship between the rate of increase of r and development temperature.

In Fig. 12, the increasing rate of r can be regarded as a function of temperature as Eq. 15. If the function is defined exactly, the characteristic curve at the end of development with a complicated history of development temperature is calculable. In typical application, finite element method of analysis of development gives the estimated history of development temperature for an imaginary development unit as $T(t)$. The estimated history of development temperature can be converted to the rate of increase of r using Eq. 15, and the integration of these gives the predicted value of r as Eq. 16.

$$\frac{dr}{dt} = Q(Temp.) \tag{15}$$

$$r = \int_0^t Q(T(t))dt \tag{16}$$

The predicted values of r can be converted into the predicted characteristic curves by putting them into Eq. 10 with the known values of C and f. Such calculations are quite convenient in the design work of development systems.

Conclusion

Though some models for characteristic curves of photothermographic materials had been proposed, some problems must be solved prior to using these models in practical matters. To solve the problem, a new model using a semiempirical simulation method was found. This method gives both the fraction of silver halide grains receiving a latent image exposure and the radius of sphere of influence from the experimental characteristic curves of several development conditions. Given that values of the fraction of silver halide grains receiving a latent image exposure are intrinsic values of the film, they represent photosensitive character including fog. The value of the radius of sphere of influence indicates the degree of development, and it has a linear relationship with development time under fixed development temperature. These parameters are useful for analysis of development rate. When the parameters are fixed, exact characteristic curves of any development conditions are calculable. This simulation method is useful for analysis and design of practical photothermographic systems.

Appendix

Derivation of Eq. 1[2]

For an average exposure of q photons, and a minimum of m photons needed to generate a latent image site, the fraction of grains with a latent image of f is given by Eq. 17 that follows Poisson's distribution. The q is proportional to the fraction of photons absorbed, the number of photons per unit area, and the area to which photon arriving. So the product of a, E, and L^2 was putted in the place of q in Eq. 17, and Eq. 1 were derived.

$$f = \sum_{p=m}^{\infty} q^p \cdot \left(\frac{e^{-q}}{p!} \right) \tag{17}$$

Derivation of Eqs. 2 and 3[2]

Note: In Klosterboer's original article[2] both W_{SS} and W_{SH} were defined as *coating weight*, but in this article both W_{SS} and W_{SH} were defined as *coating weight per unit area* as used in Hirano's article.[6] Therefore related Klosterboer equations were corrected.

Number of silver halide grains in the area A was given as N_0 in Eq. 4. Content of organic silver salts per unit volume was given as W_V in Eq. 18. Volume of the sphere of influence was given as V_{SI} in Eq. 19. The amount of organic silver salts in the sphere of influence was given as W_{SI} in Eq. 20. Optical density was assumed to be proportional to W_{SI} as Eq. 21. Equations 4, 18, 19, 20, and 21 were arranged into one equation by substituting N_0, W_V, V_{SI}, and W_{SI}. Then Eq. 2 was derived.

Equation 3 was derived from the limitation of $V_{SI} \geq 0$ at $f = 1$ on Eq. 19.

$$W_V = \frac{W_{SS} \cdot A}{T \cdot A - N_0 \cdot L^3} \tag{18}$$

$$V_{SI} = N_0 \cdot f \cdot \left(\frac{4}{3} \cdot \pi \cdot r^3 - L^3 \right) \tag{19}$$

$$W_{SI} = W_V \cdot V_{SI} \tag{20}$$

$$D = K \cdot W_{SI} \tag{21}$$

Derivation of Eq. 7

Though a derivative process was not mentioned in the article,[6] the following process was assumed.

V was defined as the actual total volume of the sphere of influence from which overlap volume was already subtracted. Occupation ratio P was defined as the ratio of above V per volume of the coated layer. If new ΔN of the sphere of influence were added into the volume of the coated layer, the expected increment of V and P could be estimated as Eqs. 22 and 23. Equation 23 was arranged and integrated as Eq. 24, and Eq. 25 was derived.

In the actual total volume of the sphere of influence, the volume in which undeveloped grains were distrib-

uted was given as V_U in Eq. 26. In the total volume of the coated layer, the content of the number of undeveloped grains per volume in which they are distributed was given as P_U in Eq. 27. So the dead volume of the undeveloped grains within the sphere of influence was given as V_D in Eq. 28, and the effective volume of the sphere of influence in which developed organic silver salts exit was given as V_E in Eq. 29. The amount of developed silver was given as M in Eq. 30. Equations 25, 29 and 30 were arranged into one equation by substituting P and V_E, and the Eq. 7 was derived.

$$\Delta V = \frac{4}{3}\pi r^3 \cdot \Delta N \cdot (1-P) \tag{22}$$

$$\Delta P = \frac{\Delta V}{A \cdot T} = \frac{\frac{4}{3}\pi r^3 \cdot \Delta N \cdot (1-P)}{A \cdot T} \tag{23}$$

$$\int \frac{1}{1-P}\, dP = \int \frac{\frac{4}{3}\pi r^3}{A \cdot T} dN \tag{24}$$

$$P = 1 - \exp\left(-\frac{4}{3}\pi r^3 \frac{N}{A \cdot T}\right) \tag{25}$$

$$V_U = V - N \cdot L^3 = A \cdot T \cdot P - N \cdot L^3 \tag{26}$$

$$P_U = \frac{N_0 - N}{A \cdot T - N \cdot L^3} \tag{27}$$

$$V_D = V_U \cdot P_U \cdot L^3 = \left(A \cdot T \cdot P - N \cdot L^3\right) \frac{N_0 - N}{A \cdot T - N \cdot L^3} L^3 \tag{28}$$

$$V_E = V_U - V_D = \left(A \cdot T \cdot P - N \cdot L^3\right)\left(\frac{A \cdot T - N_0 \cdot L^3}{A \cdot T - N \cdot L^3}\right) \tag{29}$$

$$M = P_{SS} \cdot V_E \tag{30}$$

Correction of Eq. 7 by Authors

Equation 7 has an inconsistency when the volume of a sphere of influence is near to the volume of a silver halide grain. When $4/3\pi r^3$ is close to L^3, M should be close to zero. However, it does not in Eq. 7. This inconsistency takes its origin from an error in Eq. 22. Taking into account the volume of silver halide grains, the equation was corrected as Eq. 22'. Consequently Equation 7 was corrected as Eq. 7'.

$$\Delta V = \left(\frac{4}{3}\pi r^3 - L^3\right) \cdot \Delta N \cdot (1-P) \tag{22'}$$

$$M = P_{SS}\left[AT\left\{1 - \exp\left(-\left(\frac{4}{3}\pi r^3 - L^3\right)\frac{N}{AT}\right)\right\} - NL^3\right] \left(\frac{AT - N_0 L^3}{AT - NL^3}\right) \tag{7'}$$

Derivation of Eq. 8

The shadow area of a developed silver particle S_0 is assumed to be proportional to the 2/3 power of the volume of a developed silver particle V_0 as Eq. 31. Considering covering power, the image density D is assumed to be proportional to the total shadow area of developed silver particles per unit area as Eq. 32. Equations 31 and 32 were arranged into one equation, Eq. 33, then Eq. 8 was derived.

$$S_0 = C_1 \cdot V_0^{\frac{2}{3}} = C_1 \cdot \left(\frac{M}{N}\right)^{\frac{2}{3}} \tag{31}$$

$$D = C_2 \frac{N \cdot S_0}{A} \tag{32}$$

$$D = \frac{C M^{2/3} N^{1/3}}{A} \quad \text{when } C \equiv C_1 \cdot C_2 \tag{33}$$

Acknowledgment. We thank Mr. H. Adachi for a clue to this study, and we thank for Mr. A. Nishijima and Mr. H. Yanagisawa for experimental assistance. We also thank Mr. A. Taguchi, Mr. H. Okabe and Mr. M. Sumi for preparation of the development unit, and we thank Mr. H. Takiguchi and Mr. H. Ohtani for helpful discussions.

References

1. D. H. Klosterboer and R. L. Rutledge, in *Paper Summaries, SPSE 33rd Annual Conferences,* SPSE, Washington, DC, 1980, paper N–7.
2. D. H. Klosterboer, *Imaging Processes and Materials, Neblette's Eighth Edition*, J. M. Sturge, V. Walworth, and A. Shepp Eds., Van Nostrand Reinhold, New York, 1989, p. 279.
3. C. Zou, M. R. V. Sahyun, B. Levy and N. Serpone, *J. Imaging Sci. Technol.* **40**, 94 (1996).
4. K. R. C. Gisser, in *Proc. IS&T's 49th Annual Conference*, IS&T, Springfield, VA, 1996, p. 432.
5. S. H. Kong, in *Proc. IS&T's 50th Annual Conference*, IS&T, Springfield, VA, 1997, p. 33.
6. (a) Akihiro Hirano, in *Proc. Fall Conference of SPSTJ' 97*, SPSTJ, 1997, p. 76; (b) Akihiro Hirano, in *Proc.IS&T/SPSTJ's International Symposium on Silver Halide Imaging: Recent Advances and Future Opportunities in Silver Halide Imaging,* IS&T, Springfield, VA, 1997, p. 113.
7. S. H. Kong, *J. Imaging Sci. Technol.* **43**, 509 (1999).
8. D. W. Marquardt, *J. Soc. Indust. Appl. Math.* **11**, 431 (1963).